Clean Energy, 2017, Vol. 1, No. 1, 80–89

doi: 10.1093/ce/zkx006
Advance Access Publication Date: 14 December 2017
Homepage: https://academic.oup.com/ce

RESEARCH ARTICLE

Preparation of large, ultra-flexible and free-standing nanomembranes of metal oxide–polymer composite and their gas permeation properties

Anteneh Mersha[1,2], Roman Selyanchyn[2] and Shigenori Fujikawa[1,2,3,4,*]

[1]Graduate School of Engineering, Kyushu University, Fukuoka 819-0395, Japan
[2]WPI International Institute for Carbon-Neutral Energy Research (WPI-I2CNER), Kyushu University, Fukuoka 819-0395, Japan
[3]Center for Molecular Systems (CMS), Kyushu University, Fukuoka 819-0395, Japan
[4]Laboratory for Chemistry and Life Science, Tokyo Institute of Technology, 4259 Nagatsutacho, Midori-ku, Yokohama, 226–8503, Japan

*Corresponding author. E-mail: fujikawa.shigenori.137@m.kyushu-u.ac.jp

Abstract

In this work, fabrication of free-standing nanomembranes of metal oxide (MO_x) and polymers by simple spin-coating method is discussed. First, double-layer nanomembranes containing MO_x and epoxy resin of polyethyleneimine and poly[(*o*-cresyl glycidyl ether)-co-formaldehyde] were prepared. Free-standing nanomembranes were successfully prepared, but defects formed in the metal oxide nanolayer during sharp bending of the nanomembrane. To overcome fragility of MO_x nanolayer, poly(vinyl alcohol) nanolayers were introduced between MO_x nanolayers by layer-by-layer (LbL) assembly process. The LbL nanomembrane was also free-standing and was highly flexible during macroscopic membrane manipulations. Even after transfer of the LbL nanomembrane onto a porous support, it did not have apparent cracks, confirmed by scanning electron microscopy (SEM). The LbL nanomembrane sustained low gas permeance, confirming the absence of significant defects, although it shows excellent flexibility. We believe that the presented LbL nanomembrane could be a platform useful for the design of molecular nanochannels, which is the next challenge for efficient gas separation.

Key words: nanomembranes; free-standing film; ultrathin film; layer-by-layer assembly; metal oxide; gas permeation

Introduction

Membranes have been explored as an efficient alternative for gas separation over other CO_2 capture processes, such as liquid absorption and solid adsorption, due to their lower operational energy cost [1, 2]. Organic polymeric membranes have been widely investigated to take advantage of their flexibility and solution processability [3]. However, such materials are prone to gas permeability–selectivity trade-off behavior [4, 5]. Membranes with high gas flux are strongly sought after although the gas selectivity by the current state-of-the-art membranes is satisfactory for practical use. Thinning is one of the promising approaches to improve the gas permeance of separation membranes. In biological systems, we can find molecularly thin membrane

Received: 6 March, 2017; **Accepted:** 17 October, 2017

and the lipid bilayer membrane. The lipid membrane possesses the fundamental functions as a separating system. Lipid bilayer membrane itself divides the inside and outside of a cell and has a principally barrier property for controlled molecular transport. Transmembrane proteins, such as ion transport proteins, play the main role in the transport of molecules and ions selectively. From this viewpoint, one could say that a lipid bilayer acts both as a barrier membrane and as a platform to deploy such channel proteins for energy-efficient and selective transport. By taking this essential design concept of the biological system, a less permeable membrane with nanometer thickness (nanomembrane) would be considered as a good platform useful for creating molecular channels across this nanomembrane. This is our motivation and starting point to design separation membrane with nanometer thickness.

Simple thinning often leads to membrane weakening. In polymeric membranes, fractional free volume plays an important role on molecular permeation across the membranes and, thus, controlling it is one of the issues in membrane design [5]. However, when membranes become thin, the surface property of polymers becomes different from the bulk property. For example, the surface portion of polymer films possesses lower glass transition temperature (T_g) because of the localization of its polymer chain and end groups at the surface [6–8]. This different dynamic behavior of the polymer chains near the surface may not allow the design of separation nanomembranes by simply extrapolating from the bulk properties of the polymeric membrane materials.

In contrast, metal oxide materials, such as ceramics and zeolites, have rigid molecular frameworks and, thus, one can design the size and shape of obviously-opened micropores, although the free volume spaces in polymeric membrane can be considered as a temporary pore. This rigid molecular network provides opportunities to more precisely tune molecular transport properties. For example, molecular networks in amorphous ceramic membranes can be designed by the molecular imprinting approach [9–12]. Previously, we demonstrated the facile fabrication of self-supporting ultrathin metal oxide (MO_x) films by spin coating and successfully introducing molecular channels via molecular imprinting [9]. Although selective filtration of small organic compounds dissolved in a solvent was tested, the membranes were molecular shape and size selective, which was derived from connected cavities formed during molecular imprinting. However, pure inorganic membranes are highly fragile and become more susceptible to defects when prepared in nanometer thickness. Therefore, improvement in their mechanical property remains a serious problem [3, 10].

Combining the flexibility of organic polymers and the rigidity of molecular network in inorganic materials will provide an alternative method to develop membranes and offer distinct properties different from simply adding together of original polymers and inorganics [10]. Thus, composite materials are promising for the fabrication of mechanically strong, free-standing, ultrathin membranes with the possibility to tune the molecular transport across the membrane. In addition to mechanical property, incorporation of rigid inorganic structures into the polymer matrix increases T_g [13–15], which may influence the gas transport in the composite membranes.

Various approaches, such as solution blending [16], casting [17] and layer-by-layer (LbL) assembly, have been investigated for the fabrication of composite nanomembranes [18–22]. Interest in LbL assembly has grown in the last two decades because of its simplicity, ability to control film thickness with molecular scale precision and versatility for many choices of materials architecture. Stepwise surface sol–gel fabrication of metal oxide thin films was introduced independently by Kunitake and co-workers [18] and Kleinfeld and Ferguson [21]. This is a suitable technique for the fabrication of ultrathin composite films by alternate chemisorption of molecular layers of metal oxides and polymers [19, 20]. The chemical reactions during sol–gel processing can be generally described by the following three equations [23].

$$-\mathrm{Ti}-\mathrm{OR} + \mathrm{H_2O} \rightarrow -\mathrm{Ti}-\mathrm{OH} + \mathrm{ROH} \quad \text{Hydrolysis} \tag{1}$$

$$-\mathrm{Ti}-\mathrm{OH} + \mathrm{Ti}-\mathrm{OR} \rightarrow -\mathrm{Ti}-\mathrm{O}-\mathrm{Ti}- + \mathrm{ROH} \quad \text{Condensation} \tag{2}$$

$$-\mathrm{Ti}-\mathrm{OH} + -\mathrm{Ti}-\mathrm{OH} \rightarrow -\mathrm{Ti}-\mathrm{O}-\mathrm{Ti}- + \mathrm{H_2O} \quad \text{Condensation} \tag{3}$$

As we described, a free-standing nanomembrane without severe gas leaking could become a basic platform as a membrane matrix and allow for the design and incorporation of molecular channels across the nanomembrane. With this purpose, we herein report the fabrication of stable and free-standing composite nanomembrane with low gas permeability. Although polymer–inorganic composite films have been investigated by ourselves [10, 24] and other researchers [25], the present nanomembranes are both free-standing and ultrathin. Despite its ultrathinness, the prepared composite nanomembrane showed superior mechanical flexibility. To the best of our knowledge on gas permeance properties, using such composite and free-standing nanomembranes has not been studied previously.

Two approaches for membrane preparation were investigated: surface sol–gel deposition of thin metal oxide films on a free-standing polymer nanomembrane and spin-assisted LbL assembly of alternate polymer and metal oxide layers to form double and molecular multilayers of ceramic–polymer composite nanomembranes. The LbL fabrication method was aimed to improve mechanical stability as a free-standing nanomembrane. The gas permeance properties of the fabricated nanomembranes were also tested.

1 Materials and methods

1.1 Materials

Silicon wafer with a 350-μm thickness and glass substrate were used for thin-film deposition. Poly(4-vinylphenol) (PVP, M_w = 11000, Sigma-Aldrich) and polystyrene sulfonate sodium salt (PSS, M_w = 70000, Polysciences, Inc.) were used as sacrificial layers. Poly(vinyl alcohol) (PVA, M_w = 78000, 88 mol% hydrolyzed, Polysciences, Inc.), poly[(*o*-cresyl glycidyl ether)-co-formaldehyde] (PCGF, M_w = 2500, Sigma-Aldrich) and branched polyethyleneimine (PEI, M_w = 25000, Sigma-Aldrich) were used as polymer layer precursors. Titanium *n*-butoxide (TBO, Sigma-Aldrich and Gelest Inc.), zirconium *n*-butoxide (ZBO, Kanto Chemical), aluminum s-butoxide (Gelest Inc.) and tetraetoxy silane (TEOS, Kanto Chemical) were used as metal oxide layer precursors. Ethanol (anhydrous, EMSURE, Germany), *n*-butanol, chloroform and toluene (Wako Ltd.) were used as received. All the chemicals were of analytical grade. Deionized water (18.3 MΩ cm^{-1}, Millipore, Direct-QTM) was used for washing substrate and solution preparation.

1.2 Definition of important terms

To avoid confusion with terminology, the following terms are defined:

- Membrane: a film prepared in this work that does not include the porous support.
- Free-standing nanomembrane: a nanometer-thick membrane with self-supporting property, which is capable of physically sustaining its own membrane shape without porous support.
- Porous support: a highly gas permeable physical support on to which free-standing nanomembrane is placed for a gas permeance experiment.
- Double-layer nanomembrane: a membrane that consisted of MO_x layers coated on to a polymer layer.
- Layer-by-layer (LbL) nanomembrane: a membrane comprising multiple LbL coating of MO_x–polymer.

1.3 Membrane preparation

We herein report two types of free-standing and ultrathin composite nanomembranes of metal oxide and polymers prepared by spin-coating process. Fig. 1 shows the schematic illustrations of each process.

1.3.1 *Double-layer nanomembranes of metal oxide and polymer*

To fabricate double-layer nanomembranes, we used PEI@PCGF nanomembranes as the underlayer to support MO_x layers because PCGF/PEI nanomembranes have sufficient mechanical stability to support its membrane structure without any support (Fig. 1A) [26]. Thus, the PEI@PCGF nanomembrane was firstly prepared followed by a metal oxide deposition to form double-layer nanomembranes.

(a) Polymer nanolayer

In this study, glass substrates or silicon wafers were first washed in ethanol, dried by air blowing and treated with

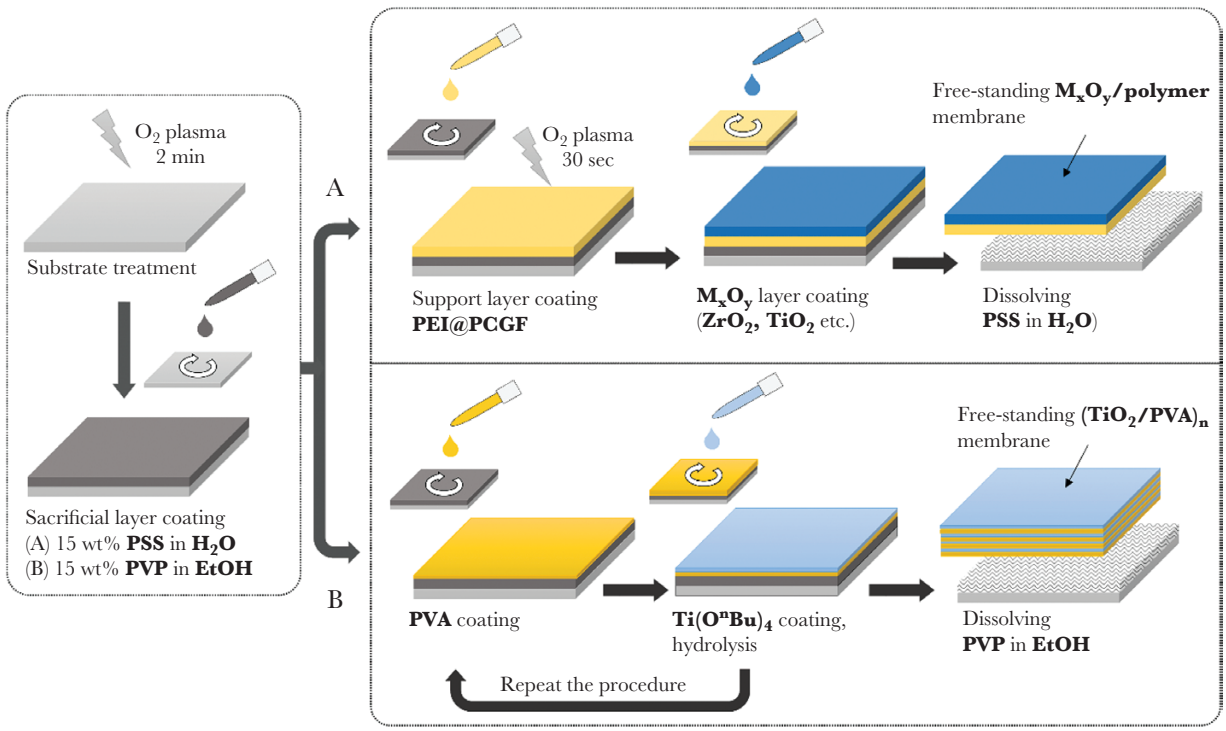

Fig. 1 The schematic representation of nanomembranes fabrication by spin-coating: deposition of MO_x layer on polymeric support (A), LbL assembly of $(PVA/TiO_2)_n$ ultrathin membrane (B)

oxygen plasma for 2 min (FA-1, SAMCO, Japan, RF power: 55 W, flow rate of oxygen: 10 sccm, chamber pressure: 20 Pa) to make the substrate surface hydrophilic with the water contact angle (WCA) of 0.3 ± 0.1°. A 15 wt% aqueous solution of PSS was spin-coated (60 s, 3000 rpm) on the glass substrate and heated at 120°C for 5 min. The mixture solution of PCGF and PEI (each 1 wt% in chloroform) was separately prepared according to the earlier report [15, 16] and it was coated over the PSS-coated glass by spin coating under the same conditions and heated at 120°C for 5 min.

(b) Metal oxide layer and film detachment

Prior to deposition of the metal oxide layer, the surface of PEI@PCGF on the substrates was treated by O_2 plasma for 30 s. The water contact angle of the PEI@PCGF layer changed from 83 ± 2° to 29.6 ± 3.9°. This plasma treatment is necessary for proper wetting by the next solution coating. Metal oxide sols were separately prepared by first dissolving corresponding metal alkoxides in 1-BuOH to obtain a 100-mM solution. Then a certain amount of 1 M HCl solution was added in the same bottle to achieve 400 mM of water which is necessary for hydrolysis of metal alkoxides. The solution was stirred for 2 h before coating. The metal oxide sols were then spin coated (60 s, 3000 rpm) on the polymer layer surface and then maintained in ambient atmosphere for at least 12 h. Free-standing and double-layer nanomembrane of MO_x–polymer were detached from the substrate by immersing the substrate in H_2O to dissolve the PSS sacrificial layer. For the gas permeance test, the membranes were transferred onto track-etched polycarbonate support (see Supplementary video S1 demonstrating detachment and transfer processes).

1.3.2 *Molecularly layered nanomembranes of TiO_2 and PVA*

A PVP layer was first deposited on a glass substrate by spin-coating (60 s, 3000 rpm) of PVP–ethanol solution (15 wt%) and aqueous PVA (0.3 wt %) was then deposited on this substrate by spin coating (2 min, 3000 rpm) (Fig. 1B). The PVA layer was allowed to dry in ambient air for 1 h. This PVA deposition introduces hydroxyl groups on the substrate and results in the formation of a well-cross-linked network of metal oxide [5]. Then, a TBO solution (50 mM, in toluene) was spin coated (2 min, 3000 rpm) and left in an ambient air for 30 min to undergo hydrolysis and condensation. This alternate sol–gel deposition cycle of PVA and TiO_2 was repeated until the desired film thickness was reached. Film growth on a quartz plate during this repetitive process was monitored by UV/Vis spectrophotometer (Jasco V-670). After dissolving the sacrificial layer of PVP in ethanol, the detached film was freely floating on an ethanol solution. It was then transferred onto an anodized porous alumina support (Anodisc, G.E. Healthcare) for surface observation and gas permeation tests.

Film thickness and surface morphology were observed using an optical microscope (Keyence VHX-600) and a field emission scanning electron microscope (FE-SEM, Hitachi S-5200).

1.4 Gas permeation experiment

Gas permeation properties of nanomembranes on a porous support were measured using a commercial instrument (GTR-11A/31A system, GTR Tec Corp., Japan) coupled to gas chromatography, as described in more details elsewhere [24]. Once the nanomembranes were prepared and transferred onto a porous support, the membrane area was fixed by Kapton and/or alumina tapes with an open hole of 1 cm diameter as shown in Fig. 2A.

Fig. 2B shows the experimental gas permeation setup. Pure and mixed gases were introduced to the feed side of the membrane cell at room temperature. The pressure of the feed gas was set at 100 kPa as a gauge pressure while the permeate side was maintained in a vacuum condition, giving a total pressure difference of ca. 200 kPa. The volume of gas passed through the membrane per unit time was measured. Gas permeance was then calculated from the measured volume.

Permeance of the gas (P) and separation factor (α) were determined according to the following equations:

$$P = N / (A \cdot \Delta P)$$

$$\alpha = P_{CO2} / P_{N2}$$

where N (in m^3/s), A (in m^2) and ΔP (in Pa) are the flow rate measured on the permeation side, effective membrane area and pressure difference, respectively. In this experiment, effective area (A) for gas permeation was 0.785 cm^2 (1 cm membrane diameter). For easier comparison, the permeance was reflected in the common GPU unit, where 1 GPU = 7.5×10^{-12} $m^3/(m^2\ s\ Pa)$.

2 Results and discussion

2.1 Double-layered nanomembranes of metal oxide and polymer

In the first trial, we have attempted to form the stable thin metal oxide layers deposited on well-established polymeric nanomembrane [27]. Fig. 3 shows the variety of metal oxide layers on PEI@PCGF. The deposition of the MO_x layer significantly reduced the macroscopic flexibility of the membrane. Thin polymeric membranes with the thickness of less than a few hundred nanometers are usually difficult to manipulate. However, the presence of the oxide layer makes the membrane stretch easily on (or in) the solvent (Fig. 3A) after the dissolution of the sacrificial layer. Due to this improved strength, it was quite easy to place such a double-layer nanomembrane on the metal frame as shown in Fig. 3B. Figs. 3C–E and G shows the cross sections of double-layer nanomembranes transferred onto a silicon wafer. In all cases, the formation of the thin and uniform double layers was clearly observed. Film thickness of the different

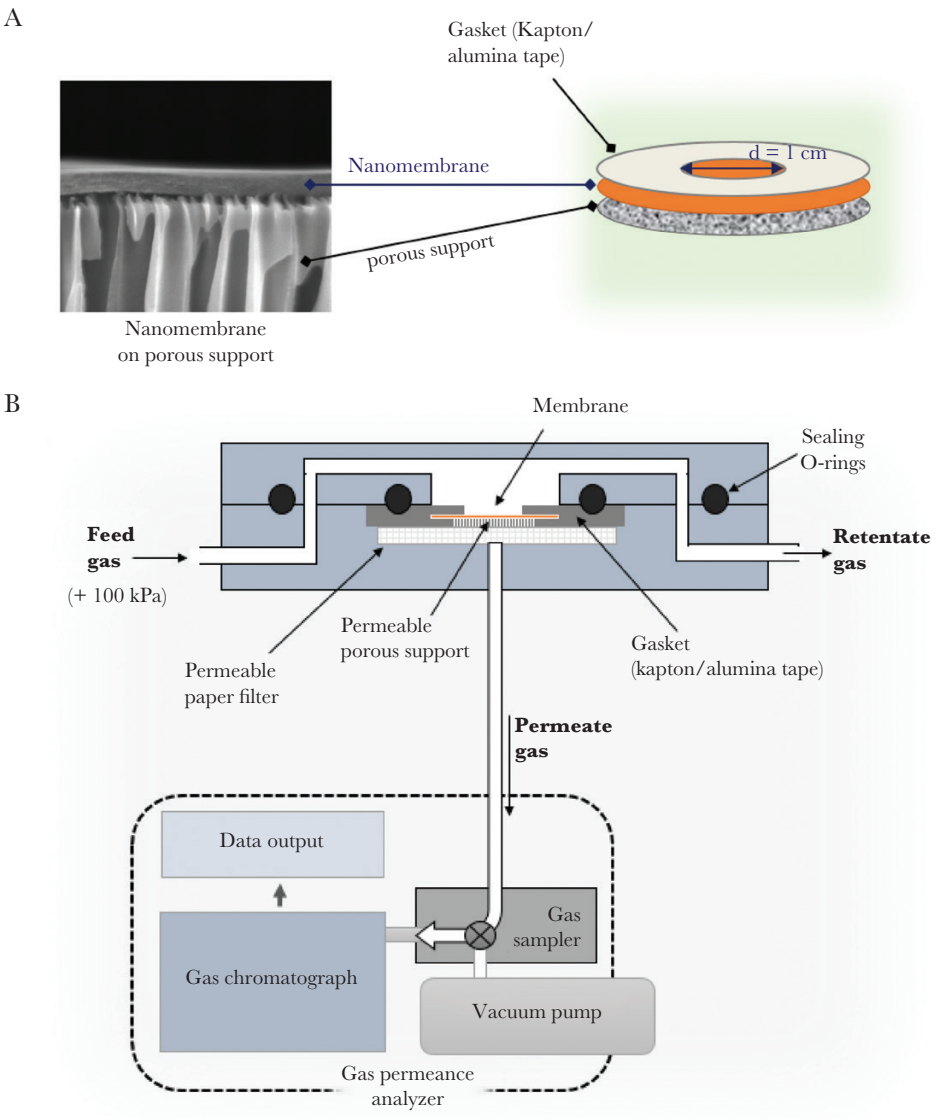

Fig. 2 A schematic representation of (A) nanomembrane assembly for gas permeation experiment and (B) gas permeance measurement apparatus

MO_x varied from 10 to 40 nm, and the thickness of polymer layer was ca. 150 nm. Sharply bent nanomembranes shown in Fig. 3C and G demonstrated that thin metal oxide (ceramic) layer could not follow the flexible bending of the PEI@PCGF layer. However, it is evident that different oxides showed different flexibility. It can be seen that the ZrO_2 layer on PEI@PCGF undergoes more damage upon membrane bending compared with mixed oxide layer ZrO_2:SiO_2 = 1:1 (Fig 3F and H, respectively). Although the mechanical properties of the double-layer nanomembranes can also be affected by the thickness of the metal oxide layer significantly, this finding may provide a way to improve and adjust the mechanical flexibility of oxide layers.

Five different gases (He, H_2, CO_2, N_2 and O_2) were used for testing the gas permeance properties of this double-layer nanomembrane. The PEI@PCGF nanomembrane with the thickness of 150 nm was chosen as a reference. Fig. 4 shows the permeance of gases relatively to their kinetic diameter. As can be seen, all membranes indeed demonstrate the selectivity towards smaller gases (helium and hydrogen) compared with gases of larger molecular sizes (CO_2, O_2 and N_2). However, the deposition of metal oxide layer resulted in increased permeance for the double-layer membrane compared with the PEI@PCGF membrane alone. Such permeance increase may be explained by the effect of oxygen plasma treatment and the solvent influence (*n*-butanol) on the polymeric layer during the spin-coating of metal oxide solution. This result is different from earlier reported deposition of TiO_2 nanolayer on PDMS (with thickness ~1 μm) where the decrease in the permeance of composite membrane was observed [24]. Most likely the observed difference may be attributed to the intrinsic properties of polymer support, i.e. PDMS is a highly permeable material while PEI@PCGF has ca. 3 orders lower permeability for CO_2 or N_2, and short treatment by 1-butanol has slightly changed the polymer matrix. An additional finding from the gas permeance

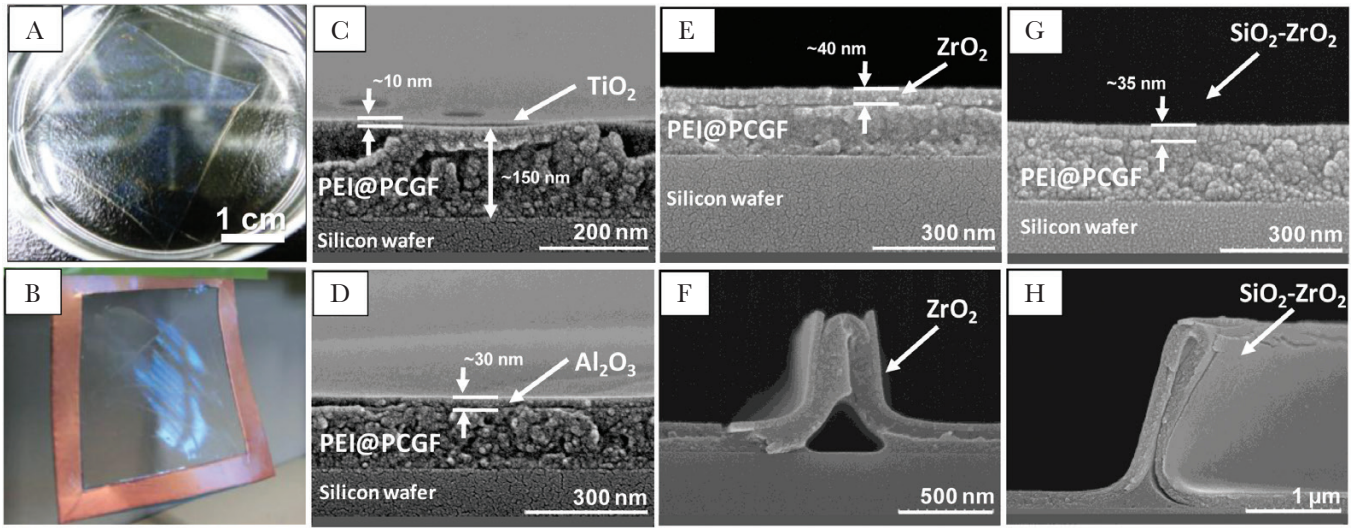

Fig. 3 Spin-coated metal oxide layers on the polymer. (A) Digital photo showing the TiO_2/PEI@PCGF membrane detached from the glass substrate freely floating on water; (B) digital photo of the composite membrane having mixed SiO_2 and ZrO_2 deposited on the PEI@PCGF membrane supported by metal frame; SEM images of the cross section of different metal oxide layers was deposited on PEI@PCGF membrane; (C) TiO_2/PCGF@PEI; (D) Al_2O_3/PCGF@PEI; (E) ZrO_2/PCGF@PEI, (G) SiO_2-ZrO_2/PCGF@PEI; (F) and (H) the bent places of the ZrO_2/PEI@PCGF and SiO_2-ZrO_2/PEI@PCGF, respectively, demonstrating that different oxides (or their mixes) provide different flexibility to the film

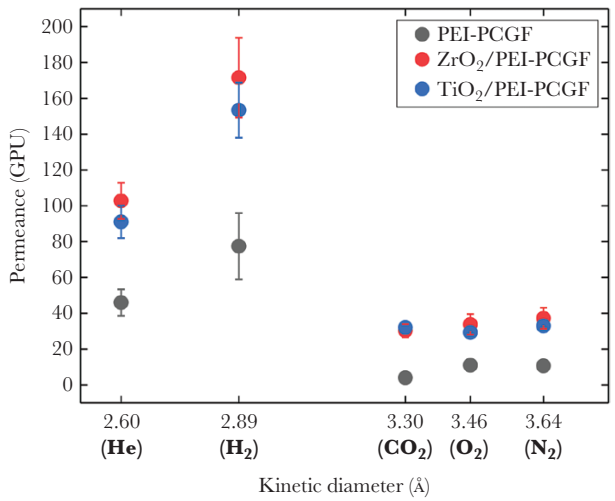

Fig. 4 Permeance of gases with different kinetic diameter through the double-layer ZrO_2/PEI@PCGF and TiO_2/PEI@PCGF nanomembranes compared with the supporting PEI@PCGF nanomembrane

data is that there is no significant difference between TiO_2 and ZrO_2 layers on the permeance or selectivity. Obviously, the chemical nature of the oxide material is quite simple and no specific interaction with gases is expected. Although the separation of different gas pairs is not extraordinary, here we demonstrate the way to assemble metal oxide films supported by organic nanomembrane. By considering the results of scanning electron microscopy (SEM), the double-layer nanomembranes may have defects even with careful manipulation of the membranes for transfer on to the porous supports. The defects may be few and insignificant because the gas permeance was not changed drastically. Despite potential defects, we believe that the usage of this membrane architecture is not completely disadvantageous. In particular, the metal oxide layer, in contrast to polymer, may work as a suitable matrix for small molecules incorporation. For example, in our previous work [24], we showed that addition of CO_2-philic component (phthalic acid) into the metal oxide layer allowed improving the selectivity toward CO_2 separation from CO_2/N_2 mixture.

2.2 LbL Nanomembranes

Defects were observed on the double-layer nanomembranes of MO_x and PEI@PCGF (Fig. 3F and H). This is due to the layers of the polymer and MO_x existing in the membrane separately, which results in an obvious ceramic nature of the MO_x layer. To overcome this fragility problem, we tried to fuse them at a molecular level by a sequential spin coating of the thin layers of the polymer and TiO_2 using the surface sol–gel process. In this case, PVA was employed as a polymer layer; since PVA has a lot of hydroxyl group at the side chain, which can react with metal alkoxides through sol–gel reaction.

UV-Vis absorbance spectra for five cycles of PVA/TiO_2 deposition is shown in Fig. 5A. The linear absorbance increases of TiO_2 at 252 nm against the cycles of deposition implied that the TiO_2 layer of similar thickness was deposited at each cycle (Fig. 5B) . The UV-Vis observation was unable to track the deposition of PVA; however, earlier works suggested that PVA is readily anchored to the titanium alkoxides due to the abundance of hydroxyl groups on its surface [28].

A highly flexible and free-standing membrane was successfully prepared after dissolving the sacrificial layer and was transferred onto a porous support. Fig. 6A demonstrates the aspiration process of a centimeter-scale membrane into a micropipette with a 2-mm diameter hole. The

detached membrane, which was floating in ethanol, was aspirated into the micropipette and released back to the solvent. The membrane undergoes multiple bending to fit the mouth of the micropipette during the sacking/release process. Once released into the solvent, the film regained its original shape and size through a simple assistance by spatula (see Supplementary video S2).

The SEM investigation showed that the fabricated nanomembrane has a smooth and uniform surface; large defects were not observed even after macroscopic manipulation. Fig. 6C and D shows the top and cross-sectional views of a 60-nm thick free-standing membrane prepared by an alternate coating of PVA and TiO_2 for 6.5 cycles (13 alternate layers), transferred onto an Anodisc. Thickness was uniform throughout the membrane. For the observed thickness, the average thickness for one cycle deposition of PVA and TiO_2 is calculated to be about 10 nm. Although layered morphologies were vaguely seen in the membrane cross section (Fig. 6D), no interspace between layers was observed, suggesting that each layer was well adhered. This result should be due to the result of interfacial sol–gel reaction between the hydroxyl groups of PVA and $Ti(O^nBu)_4$.

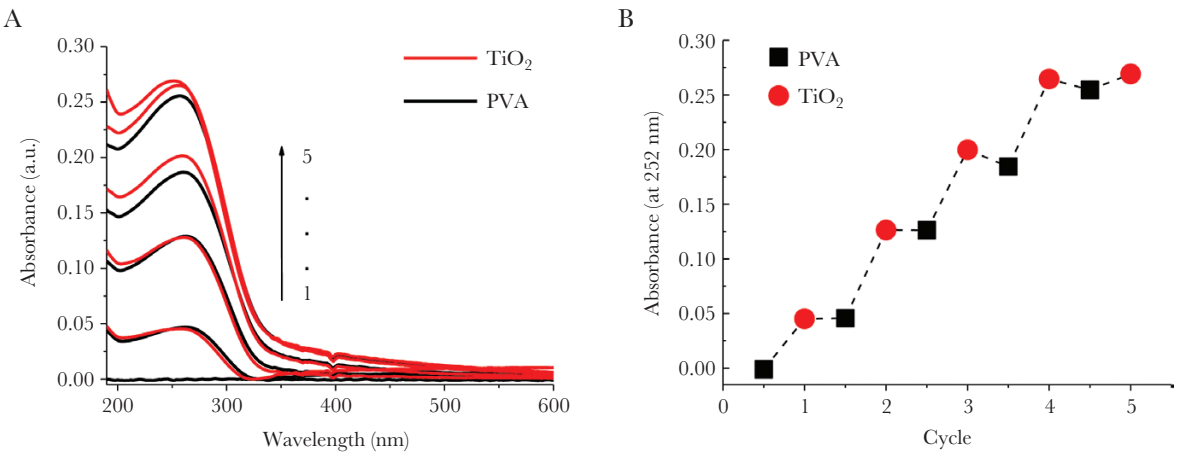

Fig. 5 (A) UV/Vis absorption spectra of sequential PVA/TiO_2 deposition, (B) UV/Vis absorbance at 252 nm of consecutive PVA and TiO_2 layers

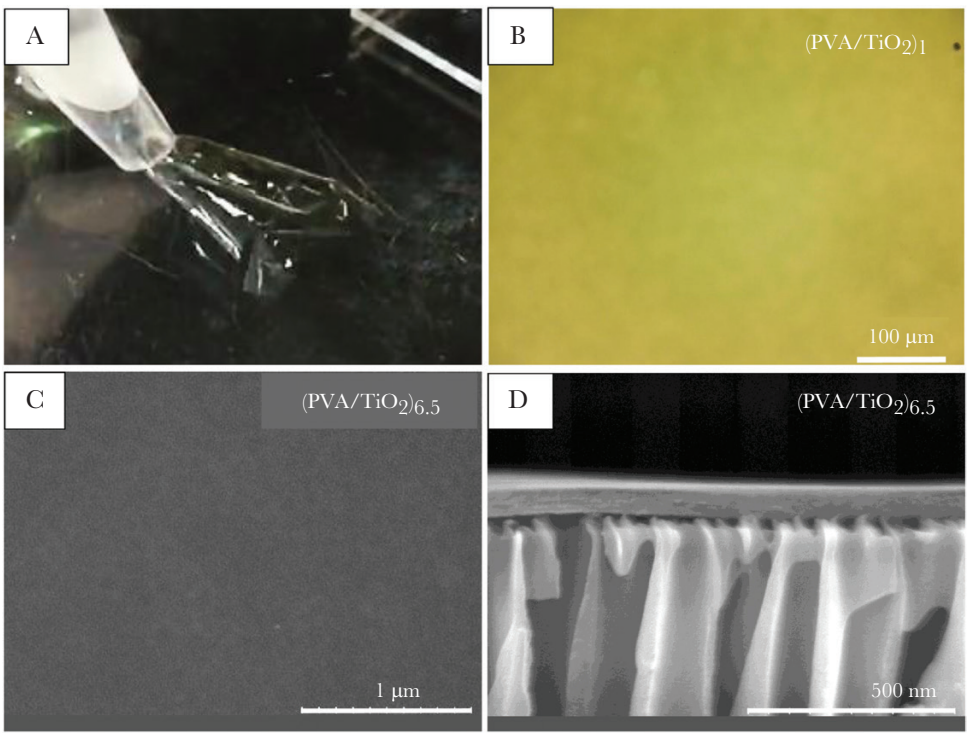

Fig. 6 LbL assembled $(PVA/TiO_2)_n$ composite nanomembrane. (A) Digital photograph showing the aspiration process of the freestanding centimeter-scale $(PVA/TiO_2)_{6.5}$ nanomembrane into a micropipette; (B) optical microscope image of the surface bi-layer PVA/TiO_2 film deposited on silicon wafer; (C) surface and (D) cross-sectional view FE-SEM images of the free-standing $(PVA/TiO_2)_{6.5}$ nanomembrane transferred onto a porous alumina (Anodisc) support

Molecular flexibility of metal oxides was discussed [29] and their intrinsic molecular flexibility contributed to the observed excellent flexibility in macroscopic scale as seen in the aspirating experiment of the LbL nanomembrane.

We could detach the LbL nanomembrane that consisted of as low as three cycles (ca. 30 nm), and successfully transferred it onto a porous support without any significant damage. Thus, incorporation of polymer network into the ceramic molecular layers by LbL assembly method, in contrast to double-layer MO_x–polymer structures, played an important role for the significant improvement of film mechanical flexibility and surface smoothness.

Gas permeation of the LbL nanomembrane with the thickness of ca. 60 nm was tested by using N_2/CO_2 (95:5) mixture gas. The membranes showed low gas permeance property (Fig. 7). TiO_2 and PVA themselves are not expected to have preferential interaction with CO_2 and N_2. Thus, we believe that this nonselective gas permeation is reasonable. In support of the SEM data, the observed small gas permeance indicated that there was no significant leakage pathway in the membrane. This LbL nanomembrane would have potential as a basic membrane matrix, which we described in the Introduction section.

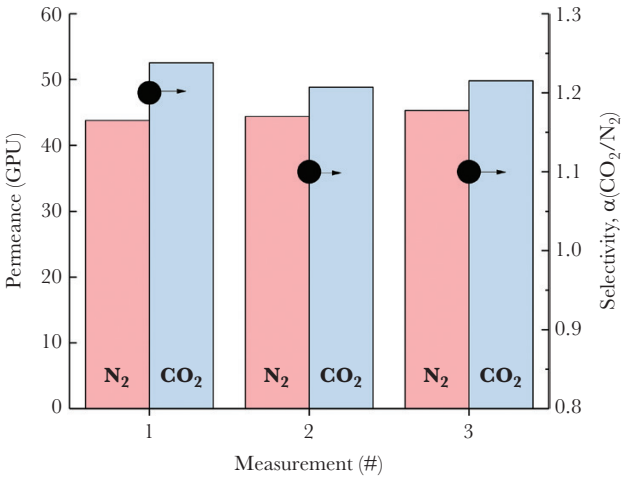

Fig. 7 Gas permeance of PVA/TiO_2 multilayer nanomembrane

3 Discussion

Fig. 8 shows the schematic illustration of the double-layer and LbL nanomembranes prepared in this work. Although the gas permeation property of the amorphous metal oxide is currently unknown, the internal structure suggests several future expectations from these nanomembranes.

In the double-layer nanomembrane, the mechanical properties of each polymer and MO_x layers may not be fused at the nanometer scale. Thus, the MO_x layer showed fragility at the nanometer scale, leading to layer breaking, although the macroscopic flexibility in the LbL membrane was improved. From this viewpoint, a molecularly layered structure in LbL nanomembrane contributes to the fusion nature of polymer and MO_x at the molecular scale. An LbL nanomembrane showed low gas permeability, which is several orders smaller compared with conventional gas separation polymer membranes. The pin-hole-free membrane was not prepared and further optimization to prepare nanomembrane with less defects is underway, and will be reported elsewhere. At the same time, the next challenge with these nanomembranes is to incorporate

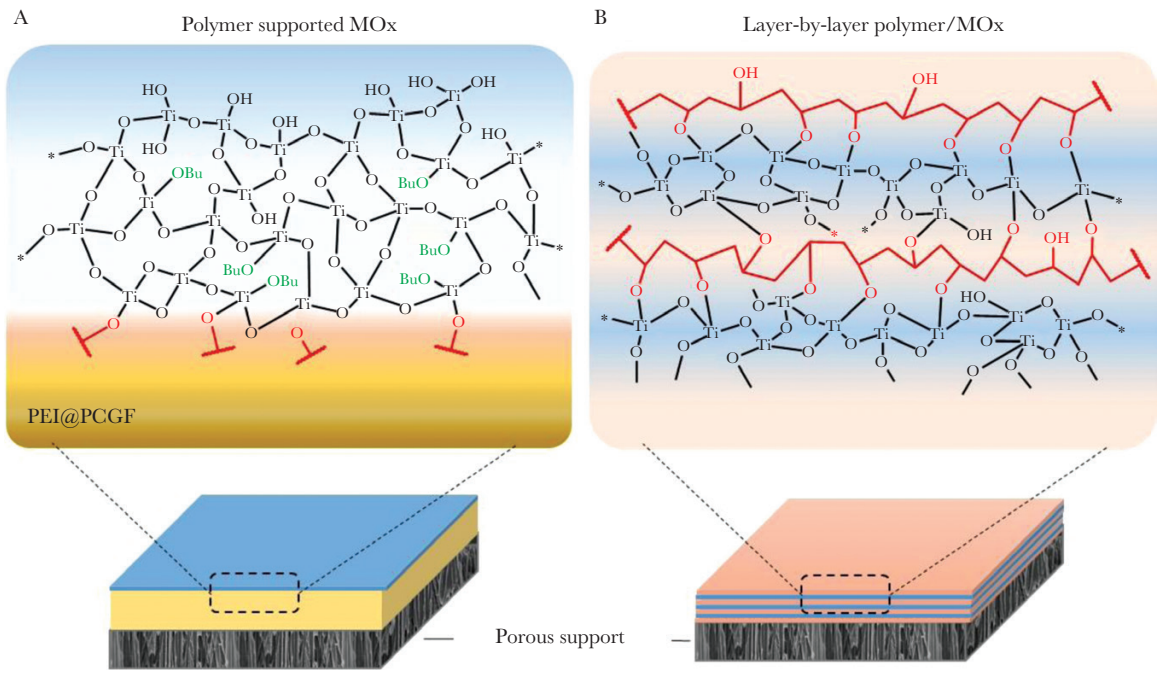

Fig. 8 Schematic representation of the internal chemical structure of metal oxide (TiO_2) layer. (A) Assembled on PEI@PCGF and (B) LbL assembled $(PVA/TiO_2)_n$ nanomembrane

(or design) nanochannels to transport gas molecules selectively. Metal oxides (in particular, TiO_2) can also be used as matrices for molecular imprinting [11, 12]. The microporosity of amorphous TiO_2 imprinted by template molecules enabled the formation of selective sites in nanomembranes. Furthermore, we reported that the incorporation of CO_2-philic compound (phthalic acid) in the TiO_2 matrix resulted in significant CO_2/N_2 selectivity improvement (α~150) [24]. This result encouraged us to design the channel structures in a nanomembrane. For the systematic investigation on the nanochannel design, the features of LbL nanomembrane without high gas selectivity could be useful to distinguish the effect of the design.

In addition, the described membranes may possess an asymmetric structure, i.e. oxide or polymer layer may be facing the gas stream first, leading to anisotropic gas separation property, depending on the feed gas direction. In the case of LbL nanomembranes having the simplest $(A/B)_n$ structure, where A and B are two different components, we can expect differences in response of $A/(B/A)_n$ and $B/(A/B)_n$ architectures. Several projects ongoing in our laboratory are investigating these and other effects of the membrane morphology on gas separation.

Therefore, we believe that amorphous metal oxide films, whether used as layers in composite membranes (once the mechanical properties improved) or as free-standing LbL nanomembranes present an interesting architecture for separation membranes in the future.

4 Conclusion

Two types of nanomembranes, MO_x–polymer double-layer nanomembrane and LbL assembly of TiO_2 and PVA, were successfully fabricated by simple spin-coating and tested for gas permeation.

Double-layer nanomembranes (MO_x–PEI@PCGF) demonstrated slightly higher permeance for five different gases compared with PEI@PCGF nanomembrane alone, without significant influence on gas selectivity. Faster gas permeation was plausibly induced by plasma treatment and solvent swelling during the oxide layer coating. SEM observation showed that the metal oxide layer cannot follow the flexibility of polymer and develop defects when the membrane is mechanically disturbed.

PVA was introduced between MO_x nanolayers by LbL assembly process to overcome fragility of the metal oxide nanolayer. The fabricated nanomembrane was free-standing and showed high flexibility without any film fragmentations during macroscopic membrane manipulations. Even after transfer of LbL nanomembranes onto a porous support, it did not have obvious cracks as confirmed by SEM observation. Nanomembrane sustained low gas permeance, confirming the absence of significant defects, although it shows excellent mechanical property.

Highly flexible and free-standing composite nanomembrane of polymers and metal oxides such as these are expected to provide great opportunities in the design of gas separation membranes as a platform for molecular nanochannel design.

Acknowledgments

This work was supported by the World Premier International Research Center Initiative (WPI), MEXT, Japan. The work was also supported by a Grant-in-Aid for Scientific Research (B) (No. 26286016), Grant-in-Aid for Scientific Research (S) (No. 25220805) from the Ministry of Education, Culture, Sports, Science, and Technology (MEXT) of Japan and a JSPS Kakenhi Grant (no. 16H06513). We gratefully acknowledge the financial support from JST ACT-C (No.24550126). The work was also supported by the Japanese government (MEXT) scholarship program and by the Japanese Society for the Promotion of Science (JSPS Grant-in-aid for Research Activity Start-up, No. 26889045).

Conflict of interest statement. The authors declare no competing financial interest.

Supplementary data

Supplementary data is available at *Clean Energy* online.

References

[1] Merkel TC, Lin H, Wei X, et al. Power plant post-combustion carbon dioxide capture: An opportunity for membranes. *J Membr Sci* 2010; 359:126–39.
[2] Liu J, Hou X, Park HB, et al. High-performance polymers for membrane CO_2/N_2 separation. *Chem Eur J* 2016; 22:15980–90.
[3] Koros WJ. Gas separation membranes: needs for combined materials science and processing approaches. *Macromol Symp* 2002; 188:13–22.
[4] Robeson LM. Correlation of separation factor versus permeability for polymeric membranes. *J Membr Sci* 1991; 62:165–85.
[5] Park HB, Kamcev J, Robeson LM, et al. Maximizing the right stuff: The trade-off between membrane permeability and selectivity. *Science* 2017; 356:1137.
[6] Kajiyama T, Tanaka K, Takahara A. Surface molecular motion of the monodisperse polystyrene films. *Macromolecules* 1997; 30:280–5.
[7] Tanaka K, Jiang X, Nakamura K, et al. Effect of chain end chemistry on surface molecular motion of polystyrene films. *Macromolecules* 1998; 31:5148–9.
[8] Tanaka K, Takahara A, Kajiayama T. Rheological analysis of surface relaxation process of monodisperse polystyrene films. *Macromolecules* 2000; 33:7588–93.
[9] Fujikawa S, Muto E, Kunitake T. Nanochannel design by molecular imprinting on a free-standing ultrathin titania membrane. *Langmuir* 2009; 25:11563–8.

[10] Kunitake T, Vendamme R, Onoue S, et al. Robust free-standing nanomembranes of organic/inorganic interpenetrating networks. *Nat Mater* 2006; 5:494–501.
[11] Araki K, Yang DH, Wang T, et al. Self-assembly and imprinting of macrocyclic molecules in layer-by-layered TiO_2 ultrathin films. *Anal Chim Acta* 2013; 779:72–81.
[12] Selyanchyn R, Lee SW. Molecularly imprinted polystyrene-titania hybrids with both ionic and π–π interactions: A case study with pyrenebutyric acid. *Microchim Acta* 2013; 180:1443–52.
[13] Li L, Chen J, Deng W, et al. Glass transitions of poly(methyl methacrylate) confined in nanopores: Conversion of three- and two-layer models. *J Phys Chem B* 2015; 119:5047–54.
[14] Pham JQ, Mitchell CA, Bahr JL, et al. Glass transition of polymer/single-walled carbon nanotube composite films. *J Polym Sci Part B Polym Phys* 2003; 41:3339–45.
[15] Askar S, Li L, Torkelson JM. Polystyrene-grafted silica nanoparticles: Investigating the molecular weight dependence of glass transition and fragility behavior. *Macromolecules* 2017; 50:1589–98.
[16] Car A, Stropnik C, Yave W, et al. PEG modified poly(amide-*b*-ethylene oxide) membranes for CO_2 separation. *J Membr Sci* 2008; 307:88–95.
[17] Scholes CA, Chen GQ, Lu HT, et al. Crosslinked PEG and PEBAX membranes for concurrent permeation of water and carbon dioxide. *Membranes* 2016; 6:0001.
[18] Ichinose I, Senzu H, Kunitake T. Stepwise adsorption of metal alkoxides on hydrolyzed surfaces: A surface sol-gel process. *Chem Lett* 1996; 25:831–2.
[19] Ichinose I, Kawakami T, Kunitake T. Alternate molecular layers of metal oxides and hydroxyl polymers prepared by the surface sol-gel process. *Adv Mater* 1998; 10:535–9.
[20] Ai S, He Q, Tian Y, et al. Fabrication of mesoporous titanium oxide nanotubes based on layer-by-layer assembly. *J Nanosci Nanotechnol* 2007; 7:2534–7.
[21] Kleinfeld ER, Ferguson GS. Stepwise formation of multilayered nanostructural films from macromolecular precursors. *Science* 1994; 265:370–3.
[22] Richardson JJ, Björnmalm M, Caruso F. Technology-driven layer-by-layer assembly of nanofilms. *Science* 2015; 348:411–21.
[23] Schubert U. Chemistry and fundamentals of the sol–gel process. In: Levy D, Zayat M, eds. *The Sol-Gel Handbook*. Germany: Wiley-VCH Verlag GmbH & Co. KGaA, 2015,3–28.
[24] Selyanchyn R, Staykov A, Fujikawa S. Incorporation of CO_2 philic moieties into a TiO_2 nanomembrane for preferential CO_2 separation. *RSC Adv* 2016; 6:88664–7.
[25] Byrd H, Holloway CE, Pogue J, et al. Ultrathin film self-assembly of hybrid organic–inorganic metal coordination polymers. *Langmuir* 2000; 16:10322–8.
[26] Watanabe H, Kunitake T. A large, freestanding, 20 nm thick nanomembrane based on an epoxy resin. *Adv Mater* 2007; 19:909–12.
[27] Fujikawa S, Ariyoshi M, Shigyo E, et al. Preferential CO_2 separation over nitrogen by a free-standing and nanometer-thick membrane. *Energy Procedia* 2017; 114:608–12.
[28] Hashizume M, Kunitake T. Preparation of self-supporting ultrathin films of titania by spin coating. *Langmuir* 2003; 19:10172–8.
[29] He J, Kunitake T. Are ceramic nanofilms a soft matter? *Soft Matter* 2006; 2:119–25.